Accepted Manuscript

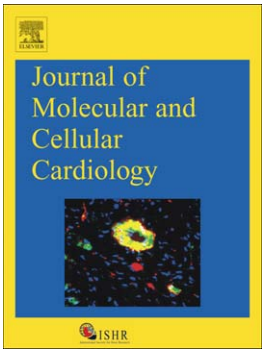

Calcium sensitivity and the Frank-Starling mechanism of the heart are increased in titin N2B region deficient mice

Eun-Jeong Lee, Jun Peng, Michael Radke, Michael Gotthardt, Henk L. Granzier

PII: S0022-2828(10)00207-5
DOI: doi: 10.1016/j.yjmcc.2010.05.006
Reference: YJMCC 6828

To appear in: *Journal of Molecular and Cellular Cardiology*

Received date: 15 January 2010
Revised date: 11 May 2010
Accepted date: 13 May 2010

Please cite this article as: Lee Eun-Jeong, Peng Jun, Radke Michael, Gotthardt Michael, Granzier Henk L., Calcium sensitivity and the Frank-Starling mechanism of the heart are increased in titin N2B region deficient mice, *Journal of Molecular and Cellular Cardiology* (2010), doi: 10.1016/j.yjmcc.2010.05.006

Calcium sensitivity and the Frank-Starling mechanism of the heart are increased in titin N2B region deficient mice.

Eun-Jeong Lee[1], Jun Peng[1,a], Michael Radke[2], Michael Gotthardt[2,3], Henk L Granzier[1,4].

[1]Department of Physiology, and [3]Department of Cell Biology and Anatomy, Sarver Molecular Cardiovascular Research Program, University of Arizona, Tucson AZ; [2]Neuromuscular and Cardiovascular Cell Biology, Max-Delbrück-Center for Molecular Medicine, Berlin, Germany, [a]present address: Department of Pharmacology, Central South University, Changsha, China; [4]Corresponding author: Henk Granzier, Dept of Physiology. University of Arizona PO Box 245217 Tucson, AZ 85724 Voice: 520-626-3641; Fax: 520-626-7600 ; Email: granzier@email.arizona.edu.

Abstract

Previous work suggests that titin-based passive tension is a factor in the Frank-Starling mechanism of the heart, by increasing length-dependent activation (LDA) through an increase in calcium sensitivity at long sarcomere length. We tested this hypothesis in a mouse model (N2B KO model) in which titin-based passive tension is elevated as a result of the excision of the N2B element, one of cardiac titin's spring elements. LDA was assessed by measuring the active tension-pCa (-log[Ca^{2+}]) relationship at sarcomere length (SLs) of 1.95, 2.10 and 2.30 μm in WT and N2B KO skinned myocardium. LDA was positively correlated with titin-based passive tension, due to an increase in calcium sensitivity at the longer SLs in the KO. For example, at pCa 6.0 the KO:WT tension ratio was 1.28 ± 0.07 and 1.42 ± 0.04 at SLs of 2.1 and 2.3 μm, respectively. There was no difference in protein expression or phosphorylation of sarcomeric proteins. We also measured the calcium sensitivity after PKA treating the skinned muscle and found that titin-based passive tension was also now correlated with LDA, with a slope that was significantly increased compared to no PKA treatment. Finally, we performed isolated heart experiments and measured the Frank-Starling relation (slope of developed wall stress-LV volume relation) as well as diastolic stiffness (slope of diastolic wall stress – volume relation). The FSM was more pronounced in the N2B KO hearts and the slope of the FSM correlated with diastolic stiffness. These findings support that titin-based passive tension triggers an increase in calcium sensitivity at long sarcomere length, thereby playing an important role in the Frank-Starling mechanism of the heart.

Keywords:

diastolic stiffness; myofilament function, passive tension; length-dependent activation

Introduction

The heart has a range of mechanisms at its disposal for adapting output, each tuned to take place at different time scales [1]. The acute systolic pressure change in response to altered venous return is known as the Frank-Starling mechanism (FSM) of the heart [2, 3]. The FSM can increase systolic pressure several-fold and is considered an indicator of the (patho)physiological state of the heart. The cellular basis of the FSM is not fully understood [2-4], but mounting evidence suggests that increased calcium sensitivity of the myofilaments in response to stretch is involved [3, 5], rather than increased calcium release [4, 6, 7]. Thus, when sarcomeres are stretched the myofilaments produce more force for the same level of calcium [2, 3, 5], i.e., the myofilaments display length-dependent activation (LDA). Multiple proteins have been proposed to mediate LDA such as the thin-filament based troponin (Tn) complex[1, 8], with a central role likely played by threonine 144 of cTnI[9], the thick-filament based proteins cMyBP-C and MLC2 [10, 11], and titin, the third myofilament of the cardiac sarcomere [8, 12-16]. Titin is an attractive candidate because it constitutes the only filament that directly senses stretch and that interacts with both actin and myosin[17]. The present study was focused on the role of titin in LDA, using a novel mouse KO model in which one of the spring elements of titin is deleted.

Titin is a giant filamentous protein that spans the half-sarcomeric distance from Z-disk to M-band[18]. Titin's I-band region functions as a molecular spring that develops passive tension when sarcomeres are stretched[19] and it is now well accepted that titin is

important for the diastolic health of the heart [17, 20-22]. The adult heart co-expresses the stiff N2B and the more complaint N2BA titin isforms [23]; passive tension can be regulated by varying the expression ratio of these two titin isoforms [24, 25], and by posttranslational modifications of titin spring elements [26-29]. A role for titin in LDA has been suggested by experiments in which titin was degraded by trypsin and LDA was reduced [12, 30], and by experiments in which changes in titin-based passive tension due to variable passive stress relaxation correlated with changes in LDA [13]. A subsequent study showed that LDA in bovine left ventricular myocardium was more pronounced than in bovine left atrial myocardium, tissues that have high and low titin-based passive tension, respectively [15]. Thus, several studies indicate a role for titin in LDA.

In the aforementioned titin studies it is difficult to exclude an additional contribution of thin and thick filament proteins, and thus determine solely the titin-based effect on LDA. To overcome this issue, we used a recently developed N2B KO mouse model in which one of the spring elements of cardiac titin (the N2B element) is excised and that as a result generates higher passive tensions [20]. Therefore, the N2B KO affords the opportunity to study the effect of increased passive tension on LDA in the same tissue type and obtain different passive tension levels that do not require trypsin treatment to degrade titin. Results show that skinned left ventricular (LV) myocardium of the N2B KO develops higher titin-based passive tension than WT myocardium, and that LDA in the N2B KO is increased. The physiological significance of our findings is supported by isolated heart experiments that revealed a more pronounced FSM in the N2B KO hearts.

Methods

Animal model. We used the N2B region-deficient mouse model (N2B KO) in which exon 49 of the titin gene has been deleted, while the remainder of the titin gene is intact [20]. Mice were genotyped as described previously [20], with the results confirmed by 1% agarose protein gels [31, 32] (Fig. 1A shows an example). Male N2B KO and WT mice (~6 month old) were anesthetized with isoflurane (Abbott Laboratories, Chicago, IL) and sacrificed by cervical dislocation. The hearts were rapidly removed, and papillary muscles from the left ventricular (LV) were dissected in oxygenated 1X HEPES (NaCl, 133.5 mM; KCl, 5mM; NaH2PO4, 1.2mM; MgSO4, 1.2mM; BDM 30 mM; HEPES, 10mM) solution. The remaining LV was quick frozen in liquid nitrogen and stored at -80°C for protein analysis. The papillary muscles were skinned in 1X relaxing solution (RS) (BES 40 mM, EGTA 10 mM, MgCl2 6.56mM, ATP 5.88 mM, DTT 1 mM, K-propionate 46.35 mM, creatine phosphate 15mM, pH 7.0) (chemicals from Sigma-Aldrich, MO, USA) with 1% Triton-X-100 (Pierce, IL, USA) overnight at ~3ºC. Muscles were then washed thoroughly with RS and stored for one month or less at -20ºC in relaxing solution containing 50% (v/v) glycerol. To prevent protein degradation, solutions contained protease inhibitors (phenylmethylsulfonyl fluoride (PMSF), 0.5mM; leupeptin, 0.04 mM; E64, 0.01 mM). Experiments were approved by the University of Arizona Institutional Animal Care and Use Committee and followed the U.S. National Institutes of Health “Using Animals in Intramural Research” guidelines for animal use.

Muscle preparations. Skinned papillary muscles were dissected into small strips (cross-sectional area (CSA) ~0.02 mm^2; length ~1.2 mm) and small aluminum clips were glued to

the ends of the muscle [33] in order to attach the muscle at one end to a force transducer (model 406, Aurora Scientific) and at the other end to a length controller (model 322C, Aurora Scientific), which were mounted on top of an inverted microscope stage. The stage contained 6 wells with different solutions in which the muscles could be placed (model 600A, Aurora Scientific). The muscles were imaged with a CCD camera, and sarcomere length was measured on-line from the striation image using a spatial autocorrelation function (model 901, Aurora scientific). The wells were temperature controlled at 15 ^{o}C. We measured the thickness and width of the preparation and, assuming an elliptical cross-section, we calculated CSA. The CSA was used to convert measured forces into tension (in mN/mm^2).

Skinned muscle solutions. We used relaxing solution (RS), pre-activating solution (Pre-A), and maximal activating solution (AS). All solutions contained the following (mM): BES, 40mM; DTT, 1 mM; creatine phosphate (PCr), 33 mM; creatine phosphokinase (CPK), 240 U/ml; the ionic strength was adjusted to 180mM with K-proprionate; pH 7.0 at 15°C.

Solution	$MgCl_2$	Na-ATP	EGTA	Ca-EGTA	K-Propionate
Relaxing	6.86	5.96	10	-	3.28
Pre-activating	6.66	5.98	1	-	30.44
Activating	6.64	6.23	-	10	2.09

The solutions contained protease inhibitors (phenylmethylsulfonyl fluoride (PMSF), 0.5 mM; Leupeptin, 0.04 mM; E64, 0.01 mM). Sub-maximal activating solutions were obtained by mixing RS and AS with the free [Ca^{2+}] calculated according to Fabiato and Fabiato [34].

Experimental Protocol. Relaxed fibers were set at a sarcomere length (SL) of 1.95 µm.

The fibers were activated in the following sequence: pre-activating solution, pCa 4.5, relaxing solution, pre-activating solution, pCa 6.05, 5.85, 5.75, 5.6, and 4.5, relaxing solution. The pCa 4.5 activation at the beginning and end were used to calculate the rundown. This sequence was carried out at three SLs: 1.95, 2.1 and 2.3 μm. For the two latter sequences the fibers were stretched (20% L_0/s), held for 5 min to allow for stress relaxation, followed by pre-activating solution and a pCa 4.5 maximal activation, and then relaxation and a release back to the slack length (see a description in Fig.3A). The protocol was then repeated except that now the muscles were exposed to progressively increasing pCa activating solutions. At the end of the third sequence the fibers were once more activated at SL 1.95 μm to obtain the rundown of the whole experiment which included three force-pCa curves (13 ± 2 % for KO (n=8) and 15 ± 2 % for WT(n=8)). Measured tensions at each sub-maximal activation were normalized by the maximal activation tension, and the normalized tensions were plotted against the pCa, to determine the tension-pCa curve. Passive tensions were measured just prior to activation. To determine titin and collagen contribution to passive tension, thick and thin filaments were extracted, removing titin's anchors in the sarcomere, by incubating the skinned muscle in relaxing solution containing 0.6 M KCl and then in relaxing solution containing 1.0 M KI for 30 min each [25]. The remaining tension, assumed to be collagen based, was subtracted from the pre-extraction tensions to determine titin-based tensions.

In a subset of experiments we studied the effect of PKA treating the skinned muscle (1hr incubation at room temperature with relaxing solution containing 1U/ul catalytic subunit of

PKA (Sigma)). We measured the force-pCa relation at SL 1.95 μm and 2.3 um before and after PKA treatment.

Analysis. The tension-pCa curves were fit to the Hill equation: T/T_{max} (relative tension) = $[Ca^{2+}]^{nH} / (K+[Ca^{2+}]^{nH})$, where n_H is the Hill coefficient, and $pCa_{50}=(-\log K)/n_H$, pCa for half-maximal activation was calculated. This pCa_{50} was used as an indicator of calcium sensitivity. For each muscle we determined the differences between pCa_{50} of the tension-pCa curves measured at SL 1.95, 2.1 and 2.3 μm and used this as an index of the length-dependent activation (i.e. $\Delta\ pCa_{50}$).

Gel-electrophoresis, Western blotting, and assessing phosphorylation. Muscle samples from left ventricular (LV) were analyzed by SDS–PAGE. Muscles were solubilized in 8M Urea buffer (8M Urea, 2M Thiourea, 3% SDS, 75mM DTT, 0.05M Tris-HCl, 0.03% bromophenol blue) and 50% glycerol with Leupeptin, E-64, and PMSF inhibitors. The protein solutions were incubated 10 min at 60°C, centrifuged for 5 min at 12,580xg to remove the particulate fraction, and then the proteins were separated by electrophoresis. For titin studies, solubilized samples were run on 1% SDS–agarose gels, electrophoresed at 15mA per gel for 3hrs and 20min, at 4°C, as previously described ([31] [32]). The gels were stained with Coomassie Blue (CB), and subsequently scanned and analyzed using One-D scan EX software (Scanalytics Inc., Rockville, MD, USA). For MHC isoform identification, 7% acrylamide (acrylamide:bis-acrylamide ratio: 37.5:1) gels were used with a 4% acrylamide stack, and gels were stained with a standard silver-stain protocol. The gels were

run for 24 hrs at 4°C and a constant voltage of 275 V. For thin-filament-based regulatory protein analyses (cTnI, cTnT, Tm-α), 12% acrylamide gels were used; for MLC-2 isoform, 15% acrylamide (acrylamide:bis-acrylamide ratio: 37.5:1) gels were used, each with a 4% acrylamide stack. The 12% and 15% acrylamide gels were run for 2hrs at room temperature at a constant voltage of 100V. For cMyBP-C isoform identification, 6% acrylamide (acrylamide:bis-acrylamide ratio: 37.5:1) gels were used with a 4% acrylamide stack, and run at room temperature for 3hrs at 50V and for another 3hrs at 100V. The same running buffer (Tris-base 0.05M, Glycine 0.384M, SDS 0.1% w/v) was used for all gels, and the cross-linker ratio of acrylamide gels was for both resolving and stacking gels 37.5:1 (Acrylamide:Bis-acrylamide).

For each protein, western blotting procedure was performed using specific antibodies (cTnI, Goat anti-cardiac TnI, Santa Cruz sc-31655; cTnT, Mouse anti-cardiac TnT, Santa Cruz sc-52285; α-Tm, Mouse anti-Tm, Hybridoma Bank CH1; cMyBP-C, Goat anti-MyBPC3, Santa Cruz sc-50115; MLC-2, Mouse anti-MLC, Sigma Aldrich M4401). Secondary antibodies conjugated with fluorescent dyes with infrared excitation spectra were used for detection. One- or two-color infrared western blots were scanned (Odyssey Infrared Imaging System, LI-COR Biosciences) and the images were analyzed. The integrated optical density of each protein expression on western blot was divided by the integrated optical density of actin on Ponseau-S stain (Sigma-Aldrich P7170) in order to normalize for loading.

In the phosphorylation studies, SDS-PAGE (4–20% acrylamide gradient) was used for

separation of myofilament proteins. The gels were fixed in 100 ml of 50% methanol and 10% acetic acid. Gels were washed three times with 100 ml of ultrapure water for 10 min each, followed by staining in 60 ml of Pro-Q Diamond (Molecular Probes; Invitrogen P33300), for 60-90 min under gentle agitation in the dark. The gels were destained 3 times, for 30 minutes each in 100ml of solution containing 20% Acetonitrile, 50mM sodium acetate, pH 4 and ultrapure water. The gels were scanned with a Typhoon 9400 (Amersham Biosciences), excitation filter 532 nm and emission filter 560 nm band pass. Then the gels were stained with Coomassie blue and scanned with an Epson Expression 1680 scanner. The images were analyzed with One-D scan EX software (Scanalytics Inc., Rockville, MD, USA). The integrated optical density of the Pro-Q diamond stain was divided by the integrated optical density of the Coomassie blue stain in order to normalize for protein loading.

Isolated Heart Experiments. An isolated heart setup was used to determine the developed and diastolic pressure to volume relationship (*P* - *V*) in hearts from N2B WT and KO mice. We used 6-month-old male KO and WT littermate mice (to ensure that the mice are as similar as possible). Mice were anesthetized (60 mg/kg sodium pentobarbitone, i.p.) and heparinized (1,000 units/kg, i.p.) followed by rapid removal of the heart and cannulation of the aorta with a blunted 17-gauge needle for retrograde coronary perfusion with oxygenated Krebs solution at a constant pressure of 80 mmHg (1 mmHg = 133 Pa) and a temperature of 37°C. A thin-walled balloon was filled with degassed water until passive pressure reached 5 mmHg. Pressure was measured with a catheter introduced into the center of the balloon. Hearts were field-stimulated at an interbeat interval of 250 ms and were beating at a baseline volume (V_{BL}) that resulted in a passive pressure of ~5 mmHg.

[Note that this is lower than the ~10Hz frequency encountered in vivo.] Single-beat analysis of LV function was performed by changing LV filling V from 90% to 125% of V_{BL} in 5% increments to generate Frank-Starling curves, and records were collected for the full set of eight commanded volumes. Pressures were measured during test beats imposed after the heart had been beating isovolumically for 30 s at V_{BL} to allow sufficient time for the preparation to stabilize fully. Diastolic pressure (P_d) was measured as the lowest LV pressure at the end of the test beat. Peak systolic pressure was measured from the test beat as well, and developed pressure (P_{dev}) was calculated as peak systolic pressure minus diastolic pressure. To account for possible changes in geometry, P was converted to wall stress (σ) by using a thick-walled spherical model: $\sigma = P/[(V_w/V + 1)2/3 -1]$, where V_w is the volume of LV wall (LV weight /1.05). The Frank-Starling protocol was run first at baseline, then the response to β-adrenergic stimulation (0.2 mM dobutamine) and β-adrenergic blockade (0.1 mM propranolol) was determined. Stable responses to dobutamine and propranolol were achieved after perfusion for 5 min each.

Statistical analysis

Data are expressed as mean ± SEM. A t-test or where appropriate ANOVA with Scheffe's posthoc test, was used with statistical significance at $p<0.05$. (Significance symbols on Figures and in Tables (*, #) one symbol: p<0.05; two symbols: p<0.01; three symbols: p<0.001). Isolated heart results were from 6 WT and 6 KO mice and skinned muscle results from 8 WT and 8 KO mice (genotypes confirmed at the protein level, see Results).

Results

We first evaluated how suitable the N2B KO model is to study the effect of titin-based passive tension on the length dependence of activation (LDA). N2B KO mice express a mutant titin that is missing the N2B element, one of the three spring elements of cardiac titin [20]. The N2B element represents ~90 kDa of protein and its absence in mutant titin is on high resolution titin gels just detectable as a titin mobility shift, relative to the mobility of WT titin, allowing us to confirm the genotype of the mice (Fig. 1A). Titin-based passive tension at SL 2.1 and 2.3 μm (measured 5 min after stretch) were significantly higher in KO mice (Fig. 1B, Table 1). Mouse myocardium also expresses a low level of N2BA titin and we determined the N2BA to N2B expression ratio in WT and KO myocardium. We found that the ratio was significantly greater in KO (0.30±0.02) than WT (0.23±0.01) myocardium (see inset of Supplementary Figure 1). The predicted effect of co-expressing N2BA titin on passive force is a small force reduction (see broken lines in Supplementary Figure 1); this reduction is much smaller than the increase in force that results from the deletion of the N2B element (Supplementary Figure 1). Because the extracellular matrix (ECM) also contributes to passive force, we measured its force contribution by extracting thick and thin filaments at the end of each experiment, thereby removing titin's anchors in the sarcomere [25]. We determined collagen-based based tension as the tension that remained after extraction: 12% (±2.2%) and 10% (±1.5%) of total passive tension was collagen-based passive tension in KO and WT (SL 2.3 μm), respectively. No significant difference existed between WT and KO mice. We also evaluated expression levels of collagens type I, III and V and included in our analysis an evaluation of the extracellular matrix protein fibronectin,

but found no difference between WT and KO myocardium (see supplementary figure 2A). This is consistent with the lack of a difference in collagen staining of histological sections (see supplementary figure 2B). Thus the main effect of the deletion of the N2B element is an increase in titin-based passive force of the N2B cardiac titin isoform.

We also evaluated expression levels and the phosphorylation status of isoforms of thin- and thick- filament proteins in N2B KO and WT myocardium, focusing on cardiac myosin binding protein-C (cMyBP-C), cardiac troponin T (cTnT), cardiac troponin I (cTnI), α-tropomyosin (α-Tm), and myosin light chain-2 (MLC-2). Antibodies to these proteins were used in a Western blot analysis, with protein loading normalized to Ponceau-S stained protein. No differences were visually detectable between WT and KO mice (Fig. 2A, left) and quantitative analysis also revealed no significant differences (Fig. 2B, left). Analysis of myosin heavy chain (MHC) isoform expression revealed that only αMHC is expressed in myocardium of KO and WT mice (Fig. 2A, bottom). The phosphorylation status of cMyBP-C, cTnT, cTnI, α-Tm and MLC-2 was assessed by Pro-Q diamond staining, a method for staining phosphoproteins (Molecular probes/Invitrogen). No obvious differences were apparent between WT and KO tissue (Fig. 2A, right). Pro-Q diamond staining was normalized to protein levels determined by staining the gels, subsequent to Pro-Q diamond staining, with Coomassie blue. This analysis revealed no significant differences between WT and KO mice (Fig. 2B, right). Thus, neither the protein levels of cMyBP-C, cTnT, cTnI, α-Tm, MLC-2, MHC nor their phosphoylation levels were altered between WT and KO mice. The only difference that was detected in the skinned myocardium of the N2B KO mice was

the smaller titin isoform. Thus it appears that the N2B KO model is well suited to study the effect of increased passive tension on LDA, without confounding changes in other myofilament proteins.

The calcium dependence of active tension development in skinned LV myocardium was measured at three different SLs: 1.95, 2.1 and 2.3 μm, using a protocol explained in Fig. 3A. The muscle was stretched in relaxing solution to a SL of either 2.1 or 2.3 μm (1.95 μm was close to the slack length (WT: 1.95 ± 0.01 μm; KO: 1.94 ± 0.01 μm) and was preset as the base length). [Note that previously we reported a reduction in slack SL in the N2B KO [20]. The lack of a difference in the present work might be due to either the different method that was used in the present work to find the slack SL (length at which preparation is just taut vs. free floating myocytes in the previous [20]) or due to the presence of ECM in the present work.] We used a constant stretch speed (20% L_0/s) and then held the muscle length constant for 9 min followed by a release back to 1.95 μm. Passive tension increased during the stretch and partially relaxed during the hold phase, due to the well-known stress relaxation phenomenon [30]. When passive tension reached a near steady level, the relaxing solution was changed first to a pre-activating solution and then to activating solutions with progressively higher levels of calcium (expressed as pCa), followed by relaxing solution and a release back to SL 1.95 μm.

The maximal active tension at pCa 4.5 increased from ~40 mN/mm^2 to ~60 mN/mm^2 when SL was increased from 1.95 to 2.3 μm with no significant differences between WT and KO

mice (Table 1). Submaximal active tensions were expressed relative to the maximal tension at pCa 4.5 and results at the three SLs are shown for WT muscle in Fig. 3B and for KO muscle in Fig. 3C. The tension-pCa curves are shifted to the left when SL is increased, i.e., calcium sensitivity is length-dependent. The Hill coefficients were slightly reduced at the longest SL (Table 1). As a measure of calcium sensitivity we determined the pCa_{50} (pCa at which tension was half of maximal); results shown in the insets of Figs. 3B and 3C and in Table 1 reveal that the KO myocardium has a significantly higher calcium sensitivity. Thus at a given submaximal calcium concentration, KO myocardium develops higher active tension. Within the physiologically important pCa range of 5.8-6.2 [35] the tension increase varied from ~20% to ~40% at SL 2.1 µm and ~20 to ~90% at SL 2.3 µm (Fig. 4). The length dependence of activation (LDA) was determined from the ΔpCa_{50}. Significantly higher ΔpCa_{50} values were obtained in the KO mice when SL was increased from either 1.95 to 2.3 or from 2.1 to 2.3 µm (Table 1). The difference in length-dependent activation at SLs 1.95 and 2.3 µm is shown in Fig. 5A. The KO mice clearly have a significantly larger left shift in the tension–pCa curve than the WT mice. Fig. 5B shows a scattergram of the LDA results (SL 1.95 to 2.3 µm) of all WT and KO preparations. LDA is significantly correlated with titin-based passive tension.

In order to rule out that the difference in LDA between WT and KO myocardium was due to a difference in baseline phosphorylation (even though the phosphorylation analysis shown above did not reveal a difference), we performed a second series of experiments in which we first measured the force-pCa relation at SL 1.95 µm and 2.3 µm (to make the protocol

doable we omitted the middle SL), PKA treated the preparation (see Methods for details), and measured again the force-pCa curves at the two SLs. PKA-induced phosphorylation did not affect the maximal active tension, however, it significantly reduced pCa_{50} at both SL1.95 and 2.3um, regardless of genotype (Table 2). Importantly, following PKA treatment, LDA (ΔpCa_{50}) was significantly greater in KO compared to WT myocardium (Table 2). A positive correlation between titin-based passive tension and LDA was found before (p<0.01) and after (p<0.01) PKA incubation (Fig. 6); the slope of the relationship was significantly higher after PKA treatment (p<0.01).

Isolated hearts were also studied and the FSM of the left ventricle (LV) was measured. Heart were constantly beating at 4 Hz, LV volume was changed during the diastolic interval, and the first beat post-volume change was analyzed (no long-term changes in posttranslational modification will have taken place yet, ensuring that we assess only the intrinsic FSM, see also Discussion). The volume was then changed back to the baseline volume and when a constant response was attained a test beat at a new volume was imposed. To account for possible differences in geometry between WT and KO hearts, LV pressures were converted to wall stress (σ), see Methods. A schematic of the setup and an example of a family of superimposed pre-and post-volume change twitches are shown in Figs. 7 A and B. Diastolic wall stress (σ_d) was determined as the lowest stress at the end of the test beat (first beat post-volume change). Developed wall stress (σ_{dev}) was calculated as peak systolic stress minus diastolic stress with measurements obtained in the presence of 0.2 mM dobutamine, or 0.1 mM propranolol. (See Discussion for details.) An example of a set of σ_{dev} – volume and σ_d – volume curves of a WT and KO heart are shown

superimposed in Fig. 7C. Both types of curves increased linearly with volume (R^2 of linear fit typically 0.99) and summarized results of the slopes of the curves (i.e., stiffness) are shown in Table 3. Under all experimental conditions, developed stiffness (i.e., the slope of the FSM) was significant larger in KO hearts (Table 2). We plotted individual results from WT and KO hearts in Fig. 7D, and this shows that developed stiffness is positively correlated with diastolic stiffness (Fig. 7D). Thus the FSM correlates with diastolic stiffness and is more pronounced in the N2B KO hearts.

Discussion

To test the role of titin in the length-dependent increase in calcium sensitivity we used a mouse model in which titin's N2B element has been deleted. The N2B element is one of the three spring elements found in cardiac titin (the PEVK and tandem Ig segments are the two other elements) [36-38]. The N2B KO myocardium develops higher titin-based passive tension than WT myocardium (Fig. 1A), which can be explained as follows. The N2B element is largely responsible for titin extension in sarcomeres longer than ~2.0 μm, (at shorter SLs, extension of the tandem Ig segments dominates, see [37]), and its absence in the KO results in a higher extension of the PEVK and tandem Ig segments [20]. Because titin-based passive tension is entropic in nature, with tension increasing with the titin fractional extension [39], the increased extension of the tandem Ig segment and PEVK region of the N2B KO mice will result in a larger titin fractional extension and hence a higher passive tension. The higher titin-based passive tension is likely to explain the increased LV diastolic stiffness in the N2B KO that was found in this study (Fig. 6B; Table 2) and the diastolic dysfunction (reduced deceleration time of the early diastolic filling E wave and a restrictive filling pattern) that was revealed in a previous echocardiography study [20]. Thus the N2B KO mouse has elevated myocardial passive tension and is therefore well suited for testing the role of titin-based passive tension in the FSM of the heart.

It is likely that the basis of the FSM is the increased myofilament calcium sensitivity at long SL [2, 3, 5], and to determine the role of titin-based passive tension in LDA we measured

force-pCa curves in skinned N2B KO and WT myocardium and evaluated LDA from the difference in the pCa_{50} values between long and short SLs. The experiments revealed significantly larger LDA in the N2B KO with a positive correlation between titin-based passive tension and LDA (Fig. 5). Because no differences were found in thin-and thick-filament protein expression or phosphorylation (Fig. 2), it is likely that the difference in LDA is due to the presence of the mutant titin isoform in N2B KO myocardium, which results in increased titin-based passive tension. Although the titin-induced shift in the force-pCa relation might be viewed as modest, its effect on active tension is large at the physiologically important pCa levels of ~6.2-5.8 [35] (average increase of 28 % at SL 2.1 µm and 51% at SL 2.3 µm).

This study can be compared with previous work on mouse skinned cardiac myocytes in which the degree of passive stress relaxation prior to activation was varied and the relationship between the level of passive tension and LDA was measured [13]. Although there are subtle differences between the results of the two studies (the pCa_{50} levels are ~0.05 units lower in single myocytes), both studies found a similar positive correlation between passive tension and LDA. This relationship between passive tension and LDA in the mouse is also similar to that obtained in a study on skinned rat trabeculae, in which titin-based passive tension was varied by trypsin-based degradation of titin [30]. Finally, a positive correlation between passive tension and LDA was found previously by comparing left ventricular and left atrial bovine myocardium, which develop high and low passive tension, respectively [15]. The present study for the first time uses a genetic model to

address the role of titin in LDA. Findings show that the N2B element is not required for LDA and that LDA is more pronounced in the N2B KO, strongly supporting the hypothesis that titin-based passive tension increases LDA.

PKA-induced phosphorylation on thin- and thick- filament based proteins is known to affect calcium sensitivity in cardiac muscle (Matsuba et al. (2010), JGP 133(6), 571-). Specifically, it has been observed in studies that PKA phosphorylation of cTnI and MyBP-C leads to lower calcium sensitivity (Cazorla et al., 2006, Cardiovascular research 69 (370-380); Kajiwara et al., 2000, Biochemical and Biophysical Research Communication 272 (104-110)). We also found a reduction in pCa50 and that the decrease was of a similar magnitude in KO and WT muscle. Importantly, after PKA phosphorylation LDA was still significantly higher in the KO (Table 2, Fig. 6). Thus titin-based passive tension correlation with LDA both before and after PKA treatment.

The mechanisms by which titin increases LDA remain to be established. Titin might affect LDA by either increasing calcium sensitivity at long SLs, or by lowering calcium sensitivity at short SLs. Cazorla et al [13] and Fukuda et al [15] obtained experimental evidence for the former, and proposed that titin-based passive tension increases calcium sensitivity at long SLs because of the compressive effect of titin-based passive tension on the spacing between thin and thick filaments. However, the work by de Tombe and colleagues has challenged the importance of lattice spacing for calcium sensitivity [2, 40, 41] and it seems worthwhile, therefore, to also consider other mechanisms. Mechanisms that have been

proposed include passive tension-based thick filament strain that promotes crossbridge interaction [13, 14] and an effect of titin on thin filament activation [9]. The latter hypothesis is supported by various studies that have established that titin interacts with the thin filament (most likely through a PEVK-actin interaction [42-44]), and if this interaction were to inhibit calcium sensitivity at short SL, while at long SL the inhibition is relieved (when strained, titin might pull away from the thin filament) the present findings could be explained. Clearly, more work is needed to understand how titin-based passive tension exerts its affect on LDA.

The physiological significance of the skinned muscle findings was addressed in isolated heart experiments. A single-beat technique was used in which a train of stable isovolumic beats is interrupted with a single perturbed beat at a new diastolic volume [45]. This protocol measures the intrinsic FSM, and avoids changes in the contractile state that occur during sustained beating at a new diastolic volume (the so-called slow force response to stretch that involves changes in phosphorylation of sarcomeric and calcium-handling proteins [46]). Because it is known that the FSM becomes steeper in response to beta-adrenergic stimulation [47, 48], and to exclude that our results are confounded by differences in beta-adrenergic 'tone' between WT and KO hearts, measurements were performed in the presence of the beta-adrenergic agonist dobutamine or antagonist propranolol. The slope of the FSM was significantly higher in the N2B KO both in the presence of dobutamine or propranolol (Table 2). The increased FSM in the N2B KO hearts and the positive correlation between the slope of the FSM and diastolic stiffness

(Fig. 7D) is consistent with the skinned muscle results and indicates that the effect of titin-based tension on calcium sensitivity plays a significant role in the FSM of the heart. This is also supported by the results of an echocardiography study which showed that N2B KO hearts are hyper-contractile and have a larger ejection fraction than WT hearts [20].

Summary. The increase in calcium sensitivity at long sarcomere length is more pronounced in skinned myocardium of the N2B KO mouse and this increase correlates with titin-based myocardial tension. Isolated heart experiments reveal that the Frank-Starling mechanism is more pronounced in the N2B KO model, supporting that the titin-based increase in calcium sensitivity is physiologically relevant. Thus, the present work supports that titin-based passive tension increases calcium sensitivity and is a contributing factor to the Frank-Starling mechanism of the heart.

Acknowledgements

We kindly thank Luann Wyly, Tiffany Pecor and Dr. Carlos Hidalgo for outstanding help. Funding by NIH grant HL62881(HG), a postdoctoral fellowship from AHA (EJL) and DFG(MG).

Captions

Figure 1. Characterization of the N2B KO mouse model. (A) Titin expression in LV myocardium of WT and N2B KO mice (1% agarose gels). WT myocardium of the mouse expresses predominately N2B titin with a small level of N2BA titin. In the KO both N2B titin and N2BA titin have a slightly higher mobility than in the WT, consistent with the excision of the N2B element. (B) Titin-based passive tension in WT and N2B KO skinned myocardium (results from 8 WT and 8 KO mice). (Tension is steady-state tension and was measured after 5 min stress relaxation.) Asterisks: comparison between KO and WT myocardium.

Figure 2. Expression level and phosphorylation status of thin- and thick- filament proteins. A) Left top: Representative Western blots (WBs) of cMyBP-C, cTnT, cTnI, α-Tm, and MLC-2 in WT and KO left ventricular (LV) myocardium. Left bottom: MHC gels loaded with WT and N2B KO LV myocardial proteins and bovine left ventricular (BLV) proteins. Right: Pro-Q diamond (Pro-Q) stained 4-20% gradient gels. B) Left: expression analysis; right: phosphorylation analysis. Protein expression levels (n=6 per genotype) and phosphorylation levels (n=8 per genotype) in KO are not significantly different from WT.

Figure 3. Force–pCa relations in WT and N2B KO skinned myocardium. (A) Explanation of experimental protocol. The preparation was stretched, held for 9 min and

then released. During the hold phase, the muscle was first in relaxing solution (pCa ~9.0), followed by pre-activating solution (Pre-A) and pCa 6.05, 5.85, 5.75, 5.6, 4.5 activating solutions, and finally relaxing solution again. Passive tension was measured just prior to activation and active tension in each activating solution was measured from the steady-state tension (arrows) minus passive tension. Active tensions were normalized by the maximal active tension at pCa 4.5. **(B and C)** Average tension-pCa curves and pCa_{50} (inset) of WT (B) and KO (C) at SL 1.95, 2.1, and 2.3 μm. In both genotypes, increasing sarcomere length left-shifts the tension-pCa curves and increases pCa_{50} values. Results from 8 WT and 8 KO mice. Asterisks: comparison between different sarcomere lengths in each genotype.

Figure 4. Tension increase in KO at submaximal calcium levels. Active tensions of KO myocardium are expressed relative to those of WT. At all pCa's (except pCa 5.5) tensions are significantly higher in KO than in WT muscles. Results from 8 WT and 8 KO mice. KO/WT ratio is significantly greater than 1 at SL2.1um (asterisks) and SL2.3um (number sign).

Figure 5. Length dependence of activation in WT and N2B KO skinned myocardium. **(A)** Average tension-pCa curves of WT (open symbols) and KO (closed symbols) at SL 1.95 and 2.3μm. Inset, ΔpCa_{50} values (asterisks: comparison between WT and KO). **(B)** ΔTitin-based passive tension is significantly correlated with LDA (ΔpCa_{50} from SL1.95 to 2.3μm) in WT (open symbols) and KO (closed symbols) myocardium. Dashed line is the

linear regression fit ($p<0.002$). Results from 8 WT and 8 KO mice

Figure 6. Length dependence of activation in WT and N2B KO skinned myocardium before and after PKA treatment. ΔTitin-based passive tension is significantly correlated with LDA (ΔpCa_{50} from SL1.95 to 2.3μm) in WT (open symbols) and KO (closed symbols) myocardium. Dashed line is the linear regression fit ($p<0.002$).

Figure 7. Assessment of FSM in isolated hearts. **(A)** Left: Schematic of isolated heart setup. The heart is perfused, twitch activated, and a small fluid-filled balloon, introduced into the LV and connected to a fast servomotor, rapidly changes LV volume; a pressure sensor inserted in the balloon measure LV pressure. **(B)** Superimposed family of set of contractions before and after (test contraction) volume change. Pressure was converted to wall stress (σ) and developed stress (σ_{dev}) and diastolic stress (σ_d) were determined. **(C)** Example of results of control (open symbols) and KO heart (closed symbols) obtained in the presence of dobutamine. Note that the developed stress (σ_{dev}) – volume relation is steeper in the KO than in the WT heart. **(D)** Developed stiffness (slope of σ - volume relation) is positively correlated with diastolic stiffness ($p<0.01$). Individual results from WT and KO hearts are shown. Inset: comparison of mean values (asterisks: comparison between WT and KO). Results from 6 WT and 6 KO mice

Supplemental Figure 1. Single molecule force-SL simulations. We calculated the force of a single N2B and a single N2BA titin molecule in WT and N2B KO mice (solid lines) and the average force of a single molecule in WT and KO sarcomere taking into account the N2BA: N2B expression ratio (inset), see broken lines. Expression of N2BA titin in a N2B dominant background reduces force, but the effect is small. The main effect of the N2B deletion is the large increase in force of the N2B titin isoform.

Details: We calculated the force—SL relations of single titin molecules using the wormlike chain WLC equation:

$$\frac{Fx(PL)}{k_B T} = \frac{z}{L} + \frac{1}{4(1 - z/L)^2} - \frac{1}{4} \qquad (1)$$

where F is force (in pN), k_B is Boltzmann's constant, T is absolute temperature, PL and L are the persistence and contour lengths. We serially-linked three WLCs, representing the combined tandem Ig segments, the PEVK, and N2B-Us spring elements. We assumed a PEVK contour length (CL) of 70 nm in N2B titin and 300 nm in N2BA titin; CL of tandem Ig segments were set at 200 nm in N2B titin and 300 nm in N2BA titin; CL of N2B Us was 200 nm for both isoforms. The assumed persistence lengths (PL) were 1.3 nm, 12 nm and 0.65 nm, respectively. We then calculated the force-SL relation of a single titin molecule and compared results for WT N2B titin, WT N2BA titin, KO N2B and KO N2BA titin and the average force-SL relation for sarcomeres that coexpress N2B and N2BA titins. For additional details on the assumed contour length, see (Trombitas et al. *Biophys J* 2000;79(6):3226-34) . For details on the assumed PL values, see Watanabe et al., *JCB*, 2002, 29;277(13):11549-58.

Supplemental Figure 2. Assessment of extracellular matrix proteins in myocardium of WT and N2B KO mice. A) Mean (±SEM) of collagen (type I, III, V) and fibronectin (FN) expression levels using qPCR (TaqMan) for N2B WT and KO mice (n=6 per genotype). Data was normalized first to 18S, and then to WT. No significant differences

were found between genotypes. **B)** Example of Trichrom staining of left ventricular myocardium from N2B WT and KO mice. N2B KO myocadium shows comparable staining of collagen (blue) with no signs of fibrosis.

References

Table 1. Mean ± SEM of passive and active tension (T) in WT and N2B KO myocardium (n=8 per genotype).

	SL (µm)	passive T (mN/mm^2)	max act.T (mN/mm^2)	ΔmaxT (%)	n_H	pCa_{50}	SL range (µm)	ΔpCa_{50}
WT	1.95	-------	42±2	------	2.7±0.06	5.71±0.02	1.95–2.1	0.09±0.01
WT	2.1	0.6±0.1	53±2	125±2	2.9±0.08	5.80±0.01	2.1–2.3	0.06±0.01
WT	2.3	3.5±0.4	60±3	142±3	2.6±0.09	5.86±0.01	1.95–2.3	0.15±0.01
KO	1.95	-------	44±3	------	2.7±0.05	5.76±0.01*	1.95–2.1	0.09±0.01
KO	2.1	1.1±0.02***	56±4	127±3	2.8±0.07	5.84±0.01*	2.1–2.3	0.10±0.01**
KO	2.3	10.7±0.4***	63±4	144±5	2.1±0.09**	5.94±0.010***	1.95–2.3	0.19±0.01***

Asterisks: comparison between KO and corresponding WT data (*t-test*); ΔMax T: maximal active tension difference from value at SL 1.95 µm; ΔpCa_{50} values apply to the SL range in the preceding column.

Table 2. Mean±SEM of passive tension (PT) and active tension (AT) in WT and N2B KO myocardium (n=5 per genotype) before and after PKA treatment.

	SL (μm)	PT (mN/mm^2)	Max AT (mN/mm^2)	n_H	pCa_{50}	ΔpCa_{50}
WT	1.95	-------	39±2	2.9±0.05	5.79±0.01	------
WT	2.3	6.6±1.5	50±3	2.2±0.11	5.92±0.02	0.13±0.01
PKA- WT	1.95	-------	41±3	2.7±0.06$^{\#}$	5.70±0.02$^{\#\#}$	------
PKA- WT	2.3	6.0±1.3$^{\#}$	52±4	2.0±0.07$^{\#}$	5.89±0.02$^{\#\#}$	0.19±0.02$^{\#}$
KO	1.95	-------	42±3	2.7±0.06	5.81±0.02	------
KO	2.3	16.5±1.1***	48±3	2.7±0.02**	6.01±0.01**	0.21±0.02**
PKA- KO	1.95	-------	42±3	2.6±0.09	5.72±0.02$^{\#\#}$	------
PKA- KO	2.3	15.0±1.1***/$^{\#\#\#}$	48±3	1.5±0.04***/$^{\#}$	5.99±0.01**/$^{\#\#}$	0.27±0.02**/$^{\#\#}$

Asterisks: comparison between KO and corresponding WT data (*t-test*);

Number sign: comparison between before and after PKA incubation;

Table 3. Mean±SEM of Diastolic and developed LV stiffness (n=6 per genotype)

	Diastolic stiffness		Developed stiffness	
Treatment	WT	KO	WT	KO
Dobutamine	2.9±0.3	6.1±0.7$^{\#\#}$	7.0±0.4	10.1±1.2 $^{\#}$
Propranolol	3.2±0.3*	6.1±0.7$^{\#}$	4.0±0.4**	5.9±0.6**/ $^{\#}$

Stiffness: slope of wall stress (in mmHg) vs. LV volume (in µl) relation; Asterisks: comparison between dobutamine and propranolol results using a paired t-test; Number sign: comparison between WT and corresponding KO result using a t-test.

[1] Solaro RJ, Rarick HM. Troponin and tropomyosin: proteins that switch on and tune in the activity of cardiac myofilaments. Journa l1998; 83: 471-80.

[2] de Tombe PP, Mateja RD, Kittipong T, Mou YA, Farman GP, Irving TC. Myofilament Length Dependent Activation. Journa.

[3] Allen DG, Kentish JC. The cellular basis of the length-tension relation in cardiac muscle. Journa l1985; 17: 821-40.

[4] Shiels HA, White E. The Frank-Starling mechanism in vertebrate cardiac myocytes. Journa l2008; 211: 2005-13.

[5] Kentish JC, ter Keurs HE, Ricciardi L, Bucx JJ, Noble MI. Comparison between the sarcomere length-force relations of intact and skinned trabeculae from rat right ventricle. Influence of calcium concentrations on these relations. Journa l1986; 58: 755-68.

[6] Allen DG, Blinks JR. Calcium transients in aequorin-injected frog cardiac muscle. Journa l1978; 273: 509-13.

[7] Allen DG, Kurihara S. The effects of muscle length on intracellular calcium transients in mammalian cardiac muscle. Journa l1982; 327: 79-94.

[8] Terui T, Sodnomtseren M, Matsuba D, Udaka J, Ishiwata S, Ohtsuki I, et al. Troponin and titin coordinately regulate length-dependent activation in skinned porcine ventricular muscle. Journa l2008; 131: 275-83.

[9] Tachampa K, Wang H, Farman GP, de Tombe PP. Cardiac troponin I threonine 144: role in myofilament length dependent activation. Journa l2007; 101: 1081-3.

[10] Cazorla O, Szilagyi S, Vignier N, Salazar G, Kramer E, Vassort G, et al. Length and protein kinase A modulations of myocytes in cardiac myosin binding protein C-deficient mice. Journa l2006; 69: 370-80.

[11] Ait Mou Y, le Guennec JY, Mosca E, de Tombe PP, Cazorla O. Differential contribution of cardiac sarcomeric proteins in the myofibrillar force response to stretch. Journa l2008; 457: 25-36.

[12] Cazorla O, Vassort G, Garnier D, Le Guennec JY. Length modulation of active force in rat cardiac myocytes: is titin the sensor? Journa l1999; 31: 1215-27.

[13] Cazorla O, Wu Y, Irving TC, Granzier H. Titin-based modulation of calcium sensitivity of active tension in mouse skinned cardiac myocytes. Journa l2001; 88: 1028-35.

[14] Fukuda N, Sasaki D, Ishiwata S, Kurihara S. Length dependence of tension generation in rat skinned cardiac muscle: role of titin in the Frank-Starling mechanism of the heart. Journa l2001; 104: 1639-45.

[15] Fukuda N, Wu Y, Farman G, Irving TC, Granzier H. Titin isoform variance and length dependence of activation in skinned bovine cardiac muscle. Journa l2003; 553: 147-54.

[16] Fukuda N, Granzier H. Role of the giant elastic protein titin in the Frank-Starling mechanism of the heart. Journa l2004; 2: 135-9.

[17] Granzier HL, Labeit S. The giant protein titin: a major player in myocardial mechanics, signaling, and disease. Journa l2004; 94: 284-95.

[18] Furst DO, Osborn M, Nave R, Weber K. The organization of titin filaments in the half-sarcomere revealed by monoclonal antibodies in immunoelectron microscopy: a map of ten nonrepetitive epitopes starting at the Z line extends close to the M line. Journa l1988; 106: 1563-72.

[19] Trombitas K, Jin JP, Granzier H. The mechanically active domain of titin in cardiac muscle. Journa l1995; 77: 856-61.

[20] Radke MH, Peng J, Wu Y, McNabb M, Nelson OL, Granzier H, et al. Targeted deletion of titin N2B region leads to diastolic dysfunction and cardiac atrophy. Journa l2007; 104: 3444-9.

[21] van Heerebeek L, Hamdani N, Handoko ML, Falcao-Pires I, Musters RJ, Kupreishvili K, et al. Diastolic stiffness of the failing diabetic heart: importance of fibrosis, advanced glycation end products, and myocyte resting tension. Journa l2008; 117: 43-51.

[22] Borbely A, Falcao-Pires I, van Heerebeek L, Hamdani N, Edes I, Gavina C, et al. Hypophosphorylation of the Stiff N2B titin isoform raises cardiomyocyte resting tension in

failing human myocardium. Journa l2009; 104: 780-6.

[23] Cazorla O, Freiburg A, Helmes M, Centner T, McNabb M, Wu Y, et al. Differential expression of cardiac titin isoforms and modulation of cellular stiffness. Journa l2000; 86: 59-67.

[24] Trombitas K, Redkar A, Centner T, Wu Y, Labeit S, Granzier H. Extensibility of isoforms of cardiac titin: variation in contour length of molecular subsegments provides a basis for cellular passive stiffness diversity. Journa l2000; 79: 3226-34.

[25] Wu Y, Cazorla O, Labeit D, Labeit S, Granzier H. Changes in titin and collagen underlie diastolic stiffness diversity of cardiac muscle. Journa l2000; 32: 2151-62.

[26] Yamasaki R, Wu Y, McNabb M, Greaser M, Labeit S, Granzier H. Protein kinase A phosphorylates titin's cardiac-specific N2B domain and reduces passive tension in rat cardiac myocytes. Journa l2002; 90: 1181-8.

[27] Fukuda N, Wu Y, Nair P, Granzier HL. Phosphorylation of titin modulates passive stiffness of cardiac muscle in a titin isoform-dependent manner. Journa l2005; 125: 257-71.

[28] Kruger M, Kotter S, Grutzner A, Lang P, Andresen C, Redfield MM, et al. Protein kinase G modulates human myocardial passive stiffness by phosphorylation of the titin springs. Journa l2009; 104: 87-94.

[29] Hidalgo C, Hudson B, Bogomolovas J, Zhu Y, Anderson B, Greaser M, et al. PKC phosphorylation of titin's PEVK element: a novel and conserved pathway for modulating myocardial stiffness. Journa l2009; 105: 631-8, 17 p following 638.

[30] Fukuda N, Wu Y, Farman G, Irving TC, Granzier H. Titin-based modulation of active tension and interfilament lattice spacing in skinned rat cardiac muscle. Journa l2005; 449: 449-57.

[31] Warren CM, Krzesinski PR, Greaser ML. Vertical agarose gel electrophoresis and electroblotting of high-molecular-weight proteins. Journa l2003; 24: 1695-702.

[32] Lahmers S, Wu Y, Call DR, Labeit S, Granzier H. Developmental control of titin isoform expression and passive stiffness in fetal and neonatal myocardium. Journa l2004; 94: 505-13.

[33] Granzier HL, Pollack GH. Effect of active pre-shortening on isometric and isotonic performance of single frog muscle fibres. Journa l1989; 415: 299-327.

[34] Fabiato A, Fabiato F. Calculator programs for computing the composition of the solutions containing multiple metals and ligands used for experiments in skinned muscle cells. Journa l1979; 75: 463-505.

[35] Gao WD, Perez NG, Marban E. Calcium cycling and contractile activation in intact mouse cardiac muscle. Journa l1998; 507 (Pt 1): 175-84.

[36] Helmes M, Trombitas K, Centner T, Kellermayer M, Labeit S, Linke WA, et al. Mechanically driven contour-length adjustment in rat cardiac titin's unique N2B sequence: titin is an adjustable spring. Journa l1999; 84: 1339-52.

[37] Trombitas K, Freiburg A, Centner T, Labeit S, Granzier H. Molecular dissection of N2B cardiac titin's extensibility. Journa l1999; 77: 3189-96.

[38] Linke WA, Stockmeier MR, Ivemeyer M, Hosser H, Mundel P. Characterizing titin's I-band Ig domain region as an entropic spring. Journa l1998; 111 (Pt 11): 1567-74.

[39] Kellermayer MS, Smith SB, Bustamante C, Granzier HL. Complete unfolding of the titin molecule under external force. Journa l1998; 122: 197-205.

[40] Konhilas JP, Irving TC, de Tombe PP. Myofilament calcium sensitivity in skinned rat cardiac trabeculae: role of interfilament spacing. Journa l2002; 90: 59-65.

[41] Konhilas JP, Irving TC, de Tombe PP. Length-dependent activation in three striated muscle types of the rat. Journa l2002; 544: 225-36.

[42] Yamasaki R, Berri M, Wu Y, Trombitas K, McNabb M, Kellermayer MS, et al. Titin-actin interaction in mouse myocardium: passive tension modulation and its regulation by calcium/S100A1. Journa l2001; 81: 2297-313.

[43] Linke WA, Kulke M, Li H, Fujita-Becker S, Neagoe C, Manstein DJ, et al. PEVK domain of titin: an entropic spring with actin-binding properties. Journa l2002; 137: 194-205.

[44] Kulke M, Fujita-Becker S, Rostkova E, Neagoe C, Labeit D, Manstein DJ, et al. Interaction between PEVK-titin and actin filaments: origin of a viscous force component in cardiac myofibrils. Journa l2001; 89: 874-81.

[45] Campbell KB, Taheri H, Kirkpatrick RD, Slinker BK. Single perturbed beat vs. steady-state beats for assessing systolic function in the isolated heart. Journa l1992; 262: H1631-9.

[46] Kockskamper J, Khafaga M, Grimm M, Elgner A, Walther S, Kockskamper A, et al. Angiotensin II and myosin light-chain phosphorylation contribute to the stretch-induced slow force response in human atrial myocardium. Journa l2008; 79: 642-51.

[47] Hanft LM, McDonald KS. Sarcomere length dependence of power output is increased after PKA treatment in rat cardiac myocytes. Journa l2009; 296: H1524-31.

[48] Sarnoff SJ. Myocardial contractility as described by ventricular function curves; observations on Starling's law of the heart. Journa l1955; 35: 107-22.

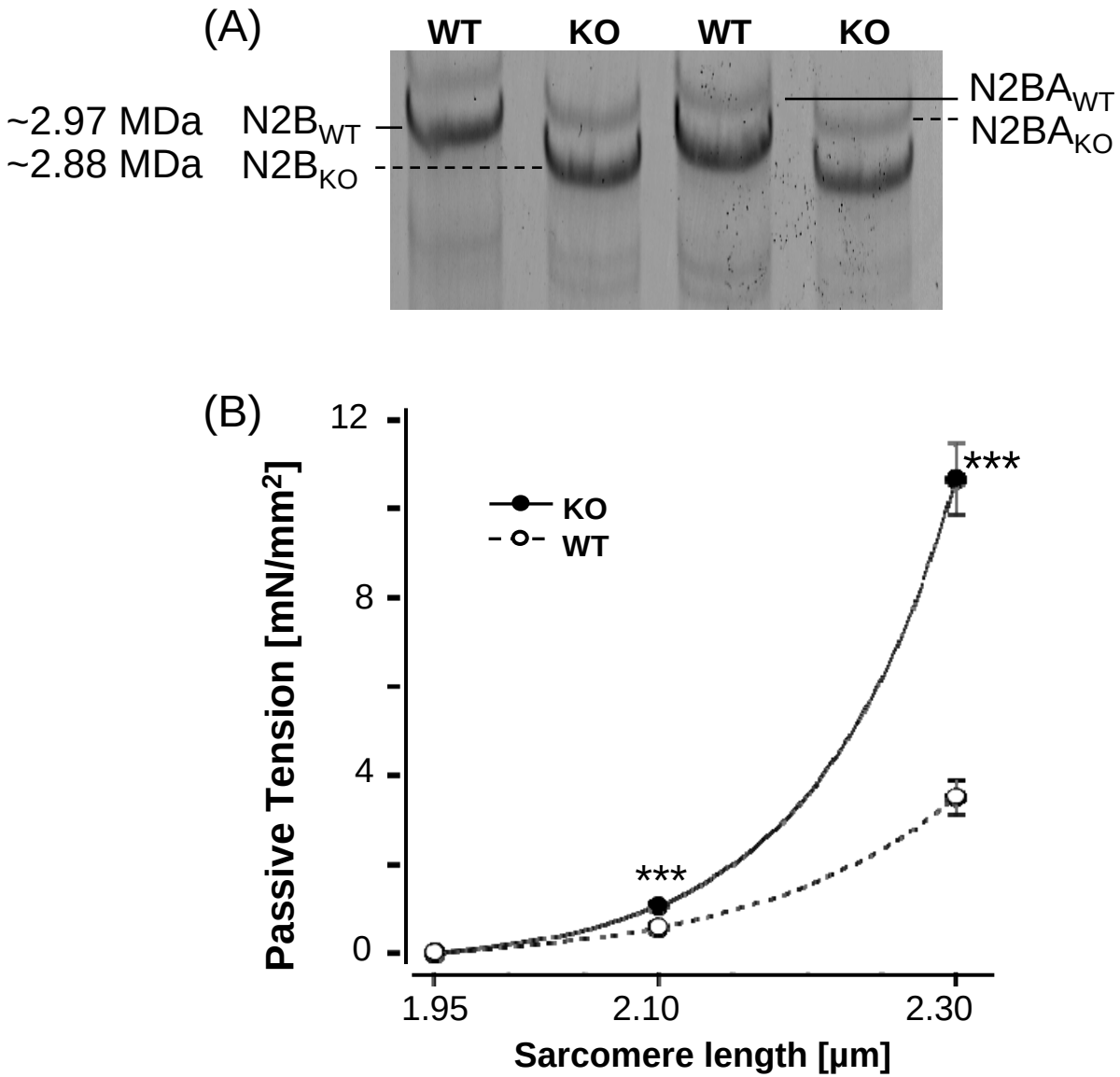

Figure 1

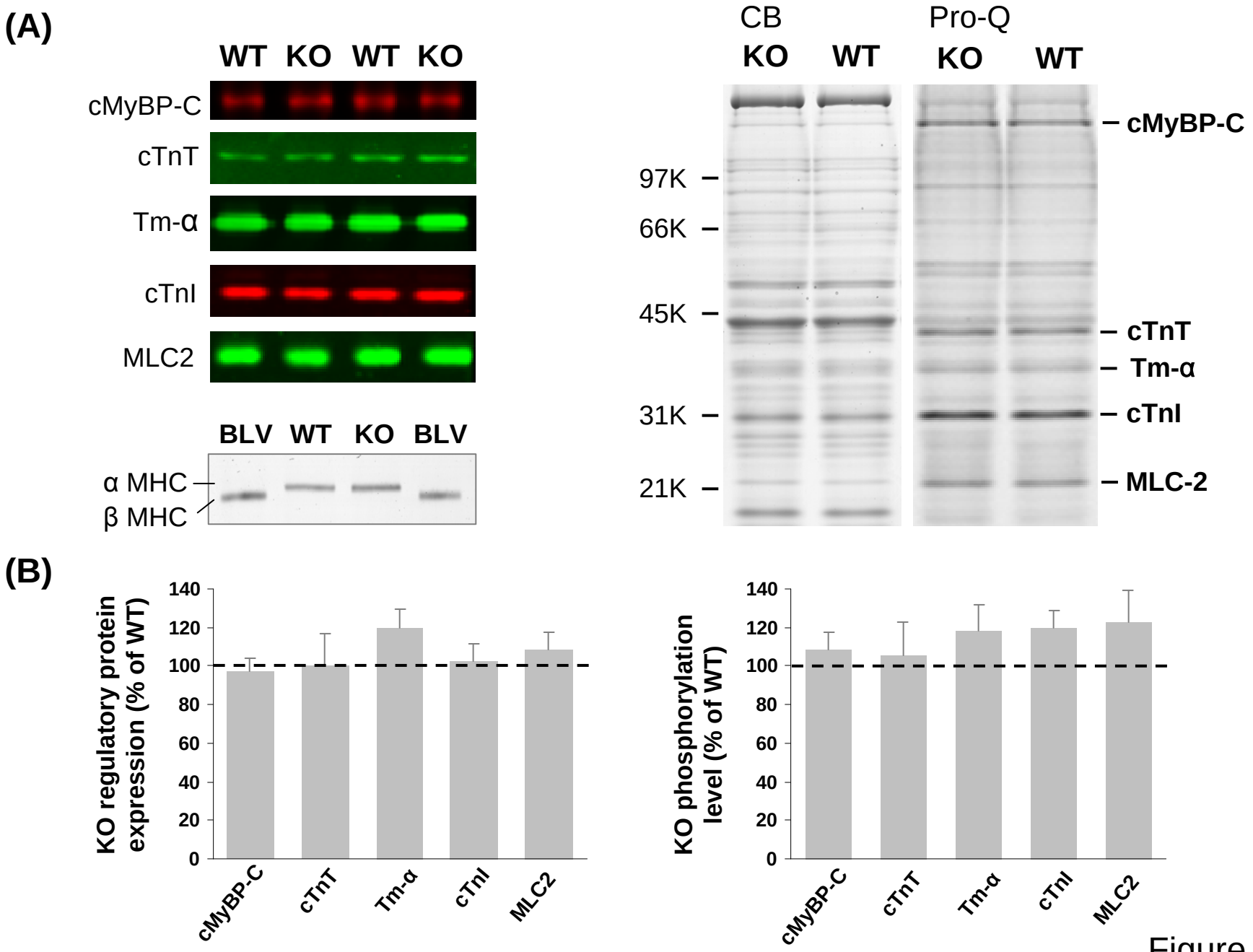

Figure 2

Figure 3

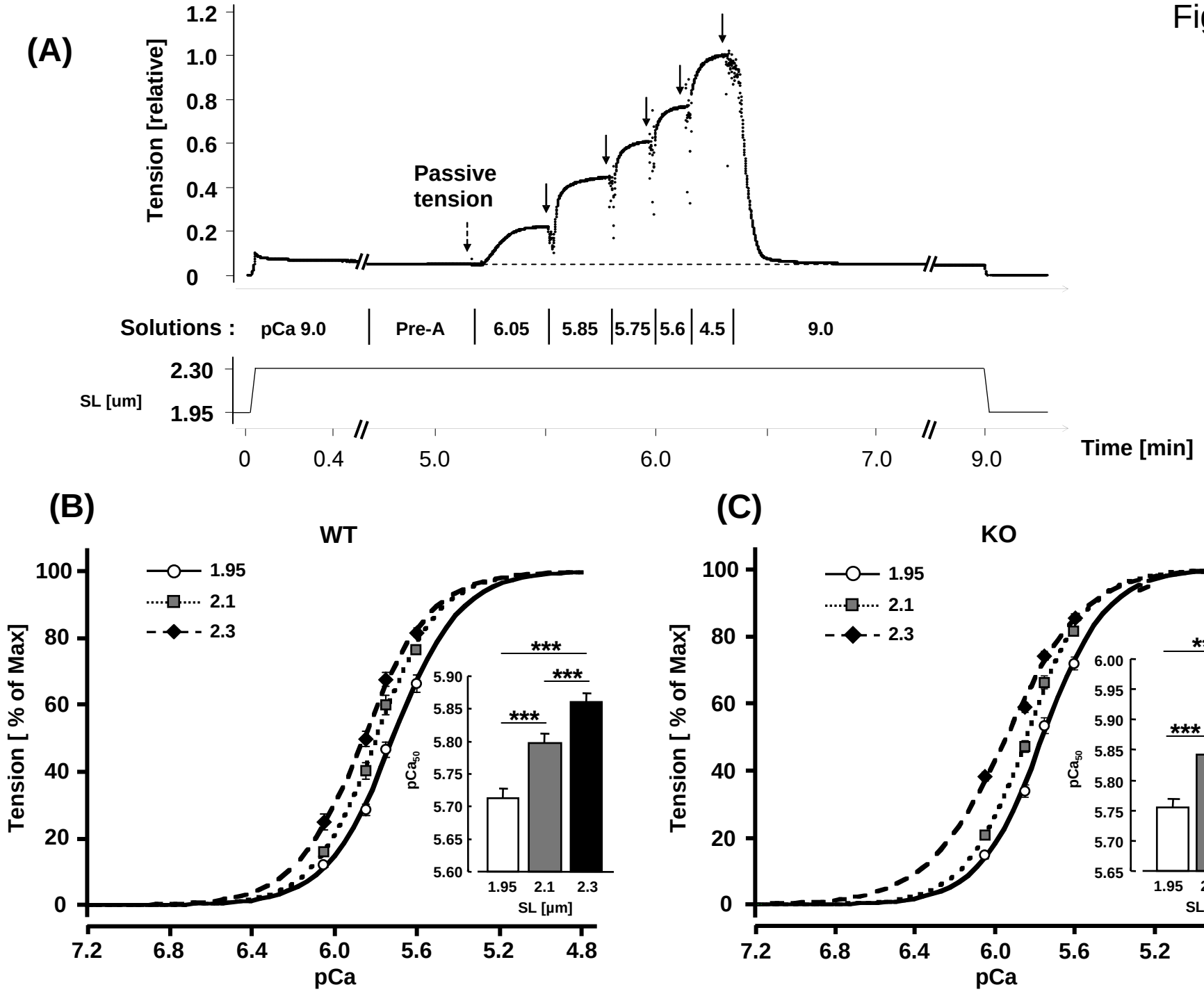

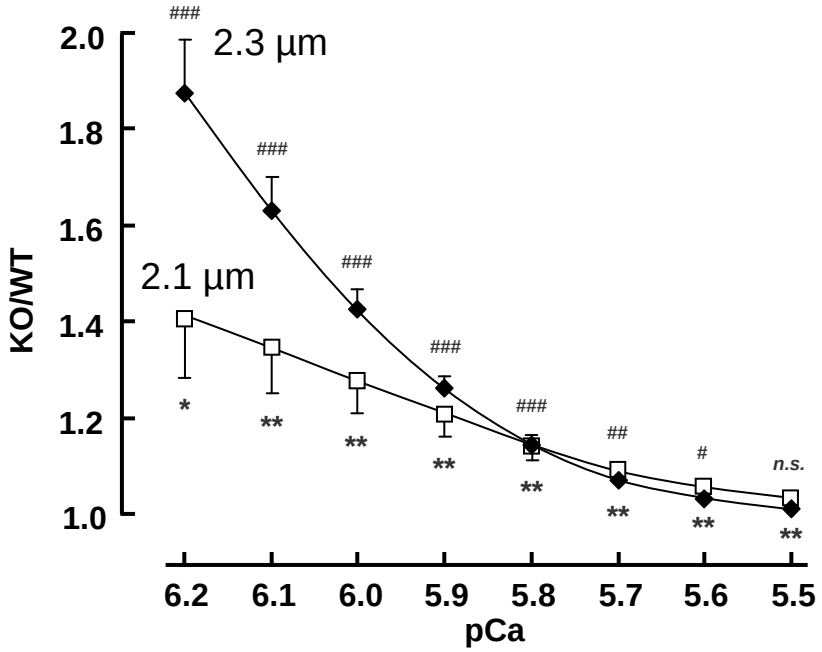

Figure 4

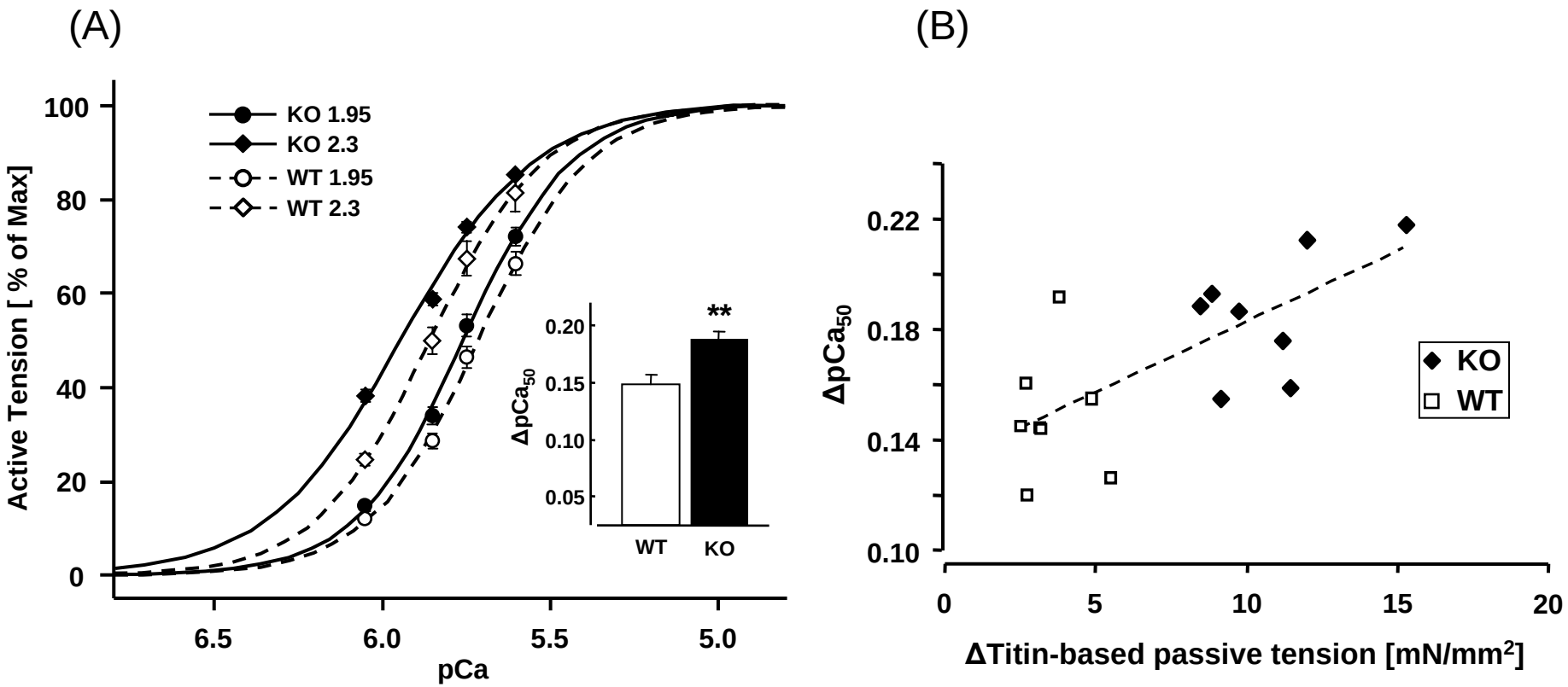

Figure 5

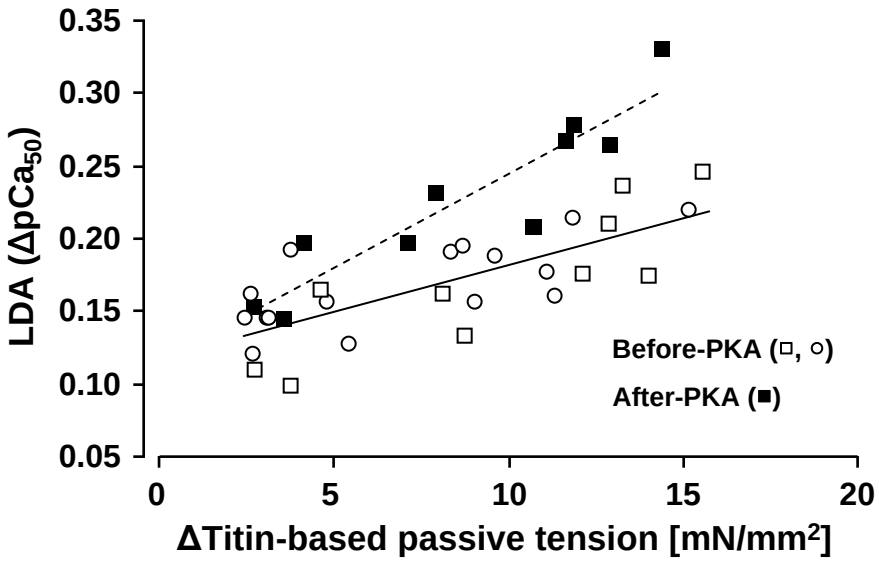

Figure 6

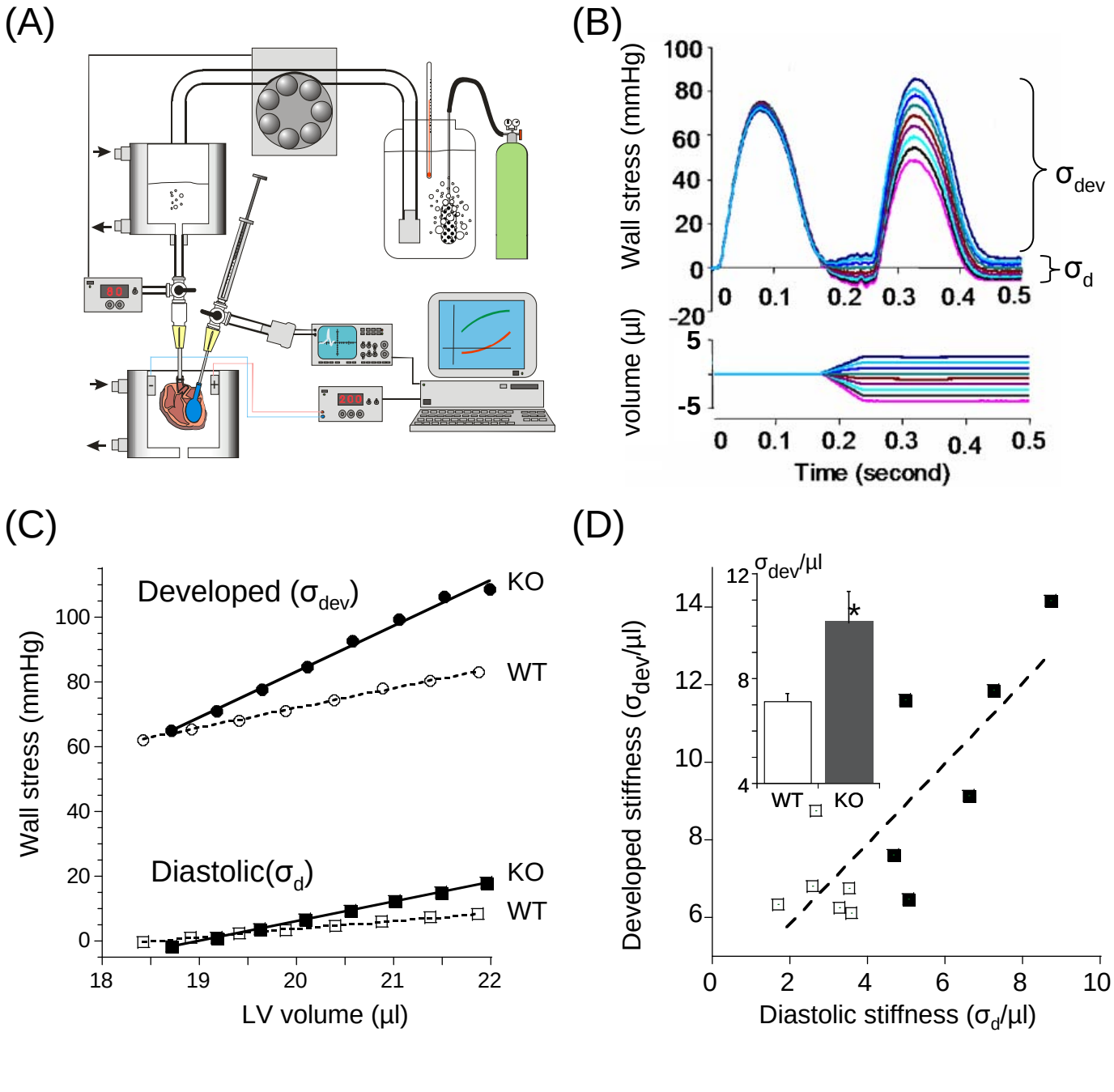

Figure 7

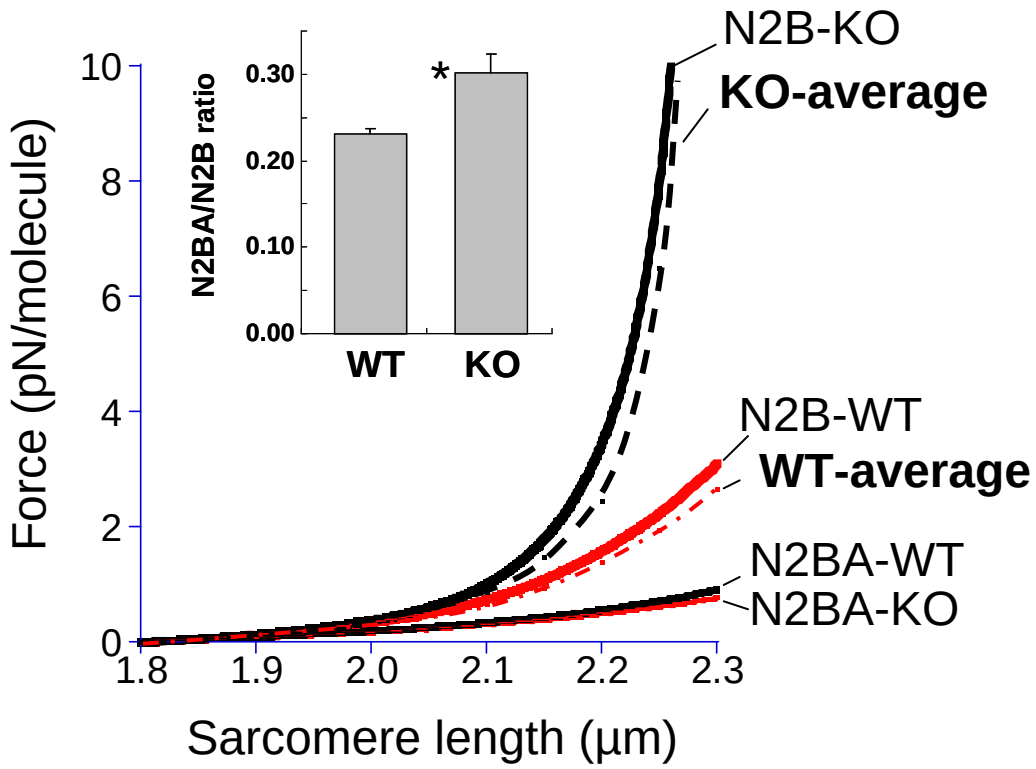

Supplemental Fig. 1

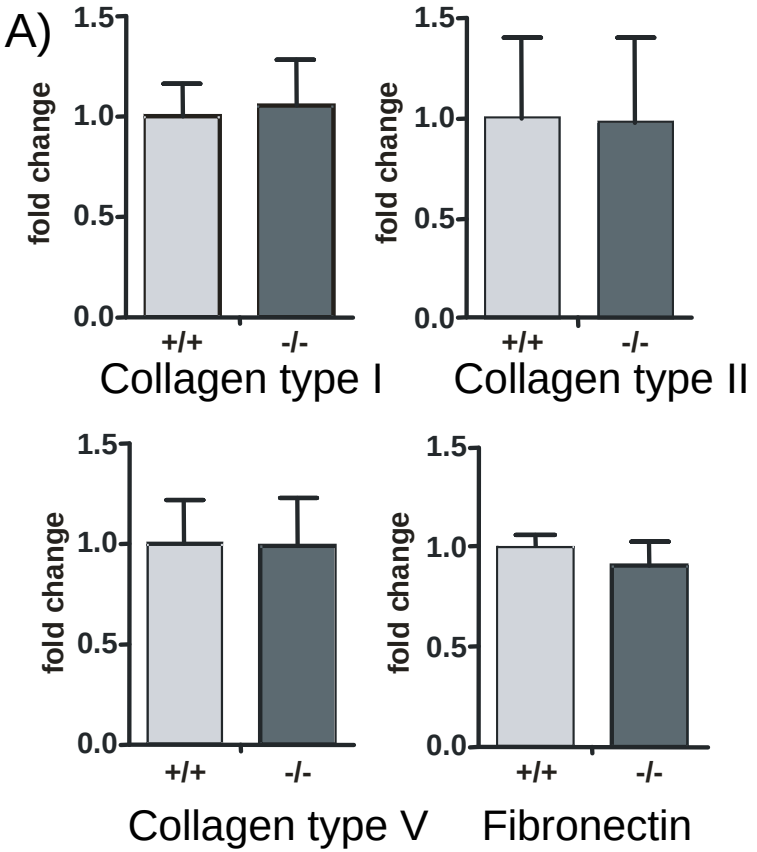

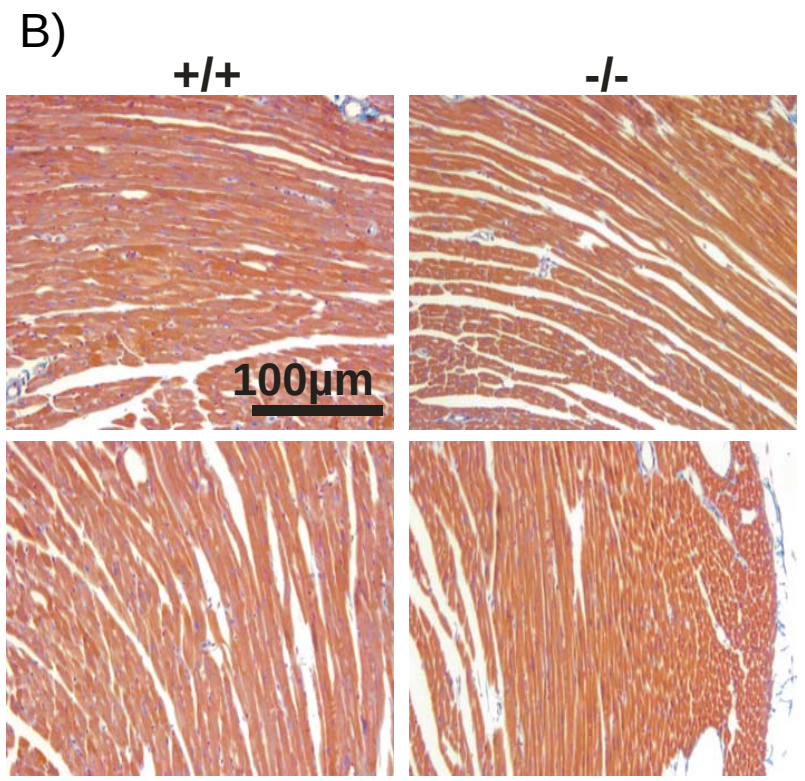

Supplemental Fig. 2